Journal of Computational Design and Engineering, 2021, 8(6), 1605–1621

https://doi.org/10.1093/jcde/qwab064
Journal homepage: www.jcde.org

RESEARCH ARTICLE

Methodology for the integration of a high-speed train in Maintenance 4.0

Alejandro Bustos*, Higinio Rubio, Enrique Soriano-Heras and Cristina Castejon

MAQLAB Research Group, Department of Mechanical Engineering, Universidad Carlos III de Madrid, Av. de la Universidad, 30, 28911 Leganes, Madrid, Spain

*Corresponding author. E-mail: albustos@ing.uc3m.es https://orcid.org/0000-0001-7513-6058

Abstract

The fourth industrial revolution is changing the way industries face their problems, including maintenance. The railway industry is moving to adopt this new industry model. The new trains are designed, manufactured, and maintained following an Industry 4.0 methodology, but most of the current trains in operation were not designed with this technological philosophy, so they must be adapted to it. In this paper, a new methodology for adapting a high-speed train to Industry 4.0 is proposed. That way, a train manufactured before this new paradigm can seize the advantages of Maintenance 4.0. This methodology is based on four stages (physical system, digital twin, information and communication technology infrastructure, and diagnosis) that comprise the required processes to digitalize a railway vehicle and that share information between them. The characteristics that the data acquisition and communication systems must fulfil are described, as well as the original signal processing techniques developed for analysing vibration signals. These techniques allow processing experimental data both in real time and deferred, according to actual maintenance requirements. The methodology is applied to determine the operating condition of a high-speed bogie by combining the signal processing of actual vibration measurements taken during the normal train operation and the data obtained from simulations of the digital twin. The combination of both (experimental data and simulations) allows establishing characteristic indicators that correspond to the normal running of the train and indicators that would correspond to anomalies in the behaviour of the train.

Keywords: Industry 4.0; Maintenance 4.0; high-speed train; railways; digital twin

1. Introduction

Traditionally, railway maintenance has been based on the performance of corrective and preventive tasks (Cheng & Tsao, 2010); therefore, the maintenance plans approved by the rolling stock manufacturers were fulfilled. This approach is a conservative strategy that can lead to unnecessary costs when replacing parts or items in good condition. In addition, complying with scheduled maintenance tasks does not eliminate the possibility of failures, as items in poor condition may not be checked.

One way to mitigate these problems is to move towards predictive or condition-based maintenance (CBM). In the scientific literature, many examples can be found focused on these types of maintenance applied to railways (Chong *et al.*, 2010; Ngigi *et al.*, 2012; Shin & Jun, 2015; Li *et al.*, 2017a; Bernal *et al.*, 2019). The researchers propose several methods for detecting failures in the railway vehicles' suspension (Li *et al.*, 2018; Lebel *et al.*, 2019; Su *et al.*, 2019), in the axle boxes (Amini *et al.*, 2016; Papaelias *et al.*, 2016; Bustos *et al.*, 2018, 2019), in the axles (Hassan

Received: 14 June 2021; **Revised:** 24 September 2021; **Accepted:** 29 September 2021

& Bruni, 2018; Gómez *et al.*, 2020), in the wheels (Li *et al.*, 2012; Alemi *et al.*, 2017; Li *et al.*, 2017b), in the braking systems (Thompson *et al.*, 2016), etc., for which vibration measurements are normally used, but also measurements from optical methods (Hyde *et al.*, 2016), ultrasounds (Dwyer-Joyce *et al.*, 2013), FBG (Lai *et al.*, 2012), etc. All kinds of signal processing techniques are applied for studying these measurements.

Despite all the scientific contributions, it was only recently that the rail industry has slowly started to adopt new maintenance methods (Alstom, 2014; Fortea, 2018; Zasiadko, 2019) and move towards Industry 4.0.

Industry 4.0 constitutes the fourth industrial revolution and is characterized by the introduction of internet-based solutions throughout the industry. It affects not only the way of designing and manufacturing but also the organization of companies and their relationship with society (Lasi *et al.*, 2014). It involves technologies such as additive manufacturing, augmented reality, digital twin, big data, artificial intelligence, data fusion, etc.

Maintenance 4.0 is also within Industry 4.0 and it takes advantage of the modern Industry 4.0 technologies to perform predictive analysis (Kans *et al.*, 2016). It is a new concept that, like everything related to Industry 4.0, is attracting the attention of researchers from all fields.

The best strategy to implement Maintenance 4.0 to predict the deterioration of systems is discussed in van Staden and Boute (2021). The paper focuses on the use of external or internal sensors and analyses different parameters (cost, reliability, etc.) to determine the advantages and disadvantages of each system. Navas *et al.* (2020) pose (from a business and theoretical point of view) all the aspects that Maintenance 4.0 should cover and how the different departments of the company involved in maintenance should be related in this new paradigm. The strengths and weaknesses of data storage systems are reviewed in Sahal *et al.* (2020) from an Industry 4.0 point of view.

Examples of the practical application of the concepts of Industry 4.0 (and Maintenance 4.0) to several sectors can also be found in the scientific literature. Saidy *et al.* (2020) implement predictive maintenance 4.0 in a complex system (desalination plant) and use the data obtained to improve the design of the system. Additive manufacturing and augmented reality are applied to aircraft maintenance (Ceruti *et al.*, 2019) to design and build optimized parts for critical systems of airliners and to help maintenance tasks in general aviation. Augmented reality is also used for supporting operation and maintenance and piping inspection in shipbuilding and offshore plants (Lee *et al.*, 2020).

Another approach is the use of reverse engineering for methods and processing techniques applied to maintenance. Two general approaches can be used for the inspection process: contact and non-contact measurements techniques. The first approach employs coordinate measuring machines (CMMs); the second approach uses a laser/optical scanner. The main approaches for reverse modelling are scattered and regular point-based methods. They differ in applicability with the varying geometric characteristics (Ke *et al.*, 2006; Xie, 2008; Urbanic & El-Maraghy, 2009; Zhao *et al.*, 2009; Urbanic, 2015; Zhang *et al.*, 2016). Reverse engineering-based methodologies have been developed and used to improve existing prototypes (Geren *et al.*, 2007). It also has been applied to develop novel machining strategies in the field of aeronautical components (Yun *et al.*, 2015). Deutsche Bahn (German national railways company) started to reverse engineer and print in 3D heavy spare parts in recent years (Zasiadko, 2019).

Focusing on railways, Kans *et al.* (2016) discuss the current situation of the Swedish railway system and how Maintenance 4.0 could help to improve it. Their work focuses mainly on traffic management and organizational effects. A new approach for track monitoring based on data fusion of signals collected in multiple trains is proposed by Lederman *et al.* (2017). A complex fuzzy system for the predictive maintenance of rails and the catenary and pantograph is proposed by Karakose and Yaman (2020). Medeiros *et al.* (2018) develop a low-cost electronic prototype to monitor the dynamics of a railway vehicle using inertial measurements. Measured data are sent to a smartphone.

The East Japan Railway Company implemented Maintenance 4.0 in recent years (Takikawa, 2016). The company followed a strategy based on four challenges or pillars: CBM, asset management, work supported by artificial intelligence, and database integration. The work exposes the case of the series E235 commuter rolling stock, which can monitor its own onboard devices and wayside equipment (track and catenary).

The railway industry is starting to apply the Digital Twin, but it is mainly oriented towards infrastructure (track, signalling, catenary, etc.) and traffic management ('In-Depth Focus: Digital Twins', 2021).

After reviewing the scientific literature, a gap between the theoretical concepts exposed and the practical implementation of Industry 4.0 in a rail vehicle is identified. To close this gap, this paper develops a new methodology for the implementation of a monitoring system based on Industry 4.0 in a high-speed train manufactured before Industry 4.0, in such a way that the new Maintenance 4.0 techniques can be used. This original methodology is conceived from a general point of view that takes into account the required aspects for implementing Maintenance 4.0: physical system, virtual system, communications, and data analysis. In addition, the data analysis is designed in such a way that it can be performed both in real time (directly on the physical system) and deferred (at the maintenance centre).

The structure of the paper is as follows: The second section presents the methodology to implement the Maintenance 4.0 system. Section 3 poses the signal processing techniques used. The fourth section discusses the results and the fifth section presents the conclusions.

2. Methodology

This section presents the proposed methodology for the integration of a high-speed train in Maintenance 4.0. The steps that make up the methodology are explained through application to a real case.

2.1. Information flow

The monitoring system is based on four main blocks and two subblocks that share information between them. These four blocks are the Physical system, the Digital Twin, the Information and Communication Technology (ICT) Infrastructure, and the Diagnosis, which can be split into short-term diagnosis and long-term diagnosis.

The relationship between the blocks is shown in Fig. 1. Solid lines represent the direct flow of information, and dashed lines represent the feedback of information.

The physical system block comprises the actual system to monitor and all the necessary equipment to carry out the measurement tasks. The digital twin is a set of virtual information that describes the actual physical system and that should be able to represent its real-time status, working condition or position (Grieves & Vickers, 2017). The ICT infrastructure block comprises the hardware and software infrastructure for transmitting,

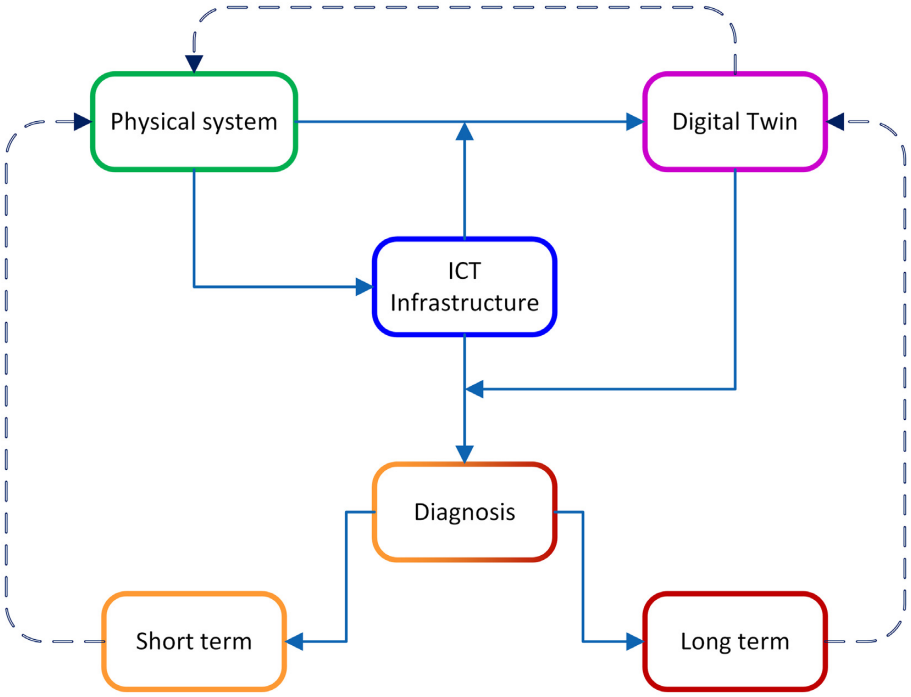

Figure 1: The flow of information in the monitoring system.

receiving, and storing the measured data. The last main block is the diagnosis block, which applies several signal processing methods to the measured data so that the condition of the physical system could be determined. According to the methods used, the diagnosis block is split into short-term diagnosis and long-term diagnosis. Short-term diagnosis involves low-computing-time techniques that can be applied in near-real time, while long-term diagnosis is oriented to study trends.

These blocks share information in the following way: The mechanical features (dimensions, weights, materials, etc.) of the physical system are used to generate the virtual model, whereas the measured data are sent to the ICT infrastructure. Measured data are also employed for updating the status of the virtual model in real time and creating the digital twin. Data stored in the ICT infrastructure are combined with information from the digital twin [e.g. finite element method (FEM) analysis]. Then, signal processing techniques are applied to the data and the diagnosis is carried out. Here, the following two options are possible:

1. On one hand, the short-term diagnosis allows detecting imminent faults in real time and, if needed, sends an alarm to the physical system so that it can be stopped before the fault takes place.
2. On the other hand, the long-term diagnosis allows studying the evolution of the physical system and to make decisions about engineering aspects of the physical system: scheduling of the maintenance plan, redesigning key parts, software upgrades, etc.

2.2. Detailed algorithm

The main blocks of the monitoring system can be split into several detail blocks, obtaining a larger and exhaustive flowchart that is shown in Fig. 2. The same colour scheme is used in both flowcharts of Figs 1 and 2: green for the physical system; purple for the digital twin and blue for the ICT infrastructure; orange for the short-term diagnosis; and red for the long-term diagnosis.

This flow chart has two starting blocks that belong to the physical system: train definition and path conditions. Then, the required measurement system is set and vibration data are acquired. These data are stored in a remote database in real time. For analysis, the data must be extracted and consolidated. These tasks are made with the help of technical documents. All these operations belong to the ICT infrastructure.

Next, in the diagnosis phase, the vibration signals are processed in the time, frequency, and time–frequency domains by using both well-known methods and new techniques. In parallel, the characterization study of the mechanical system is carried out thanks to the digital twin.

By combining the signal processing and characterization studies, a set of indicators of the train's condition will be chosen. These indicators will be the input of an intelligent system that should be able to identify the condition of the train's mechanical system automatically.

The following subsections detail the blocks of the flowchart.

2.2.1. *Physical system*

The goal of the methodology developed in this paper is to define a set of indicators that allow identifying the operating condition of a mechanical system. So it could be established if the mechanical system is working as it should be, or if a malfunction would exist, to take the respective maintenance actions. However, the first step to achieve that objective is to know the mechanical system under study (in this case, a high-speed train) and its relationship with the environment (the track).

Train definition. The first point to establish is the type of train. Different types of trains (high-speed train, intercity, commuter, freight, etc.) have diverse features and operating conditions. Hence, their performance is different.

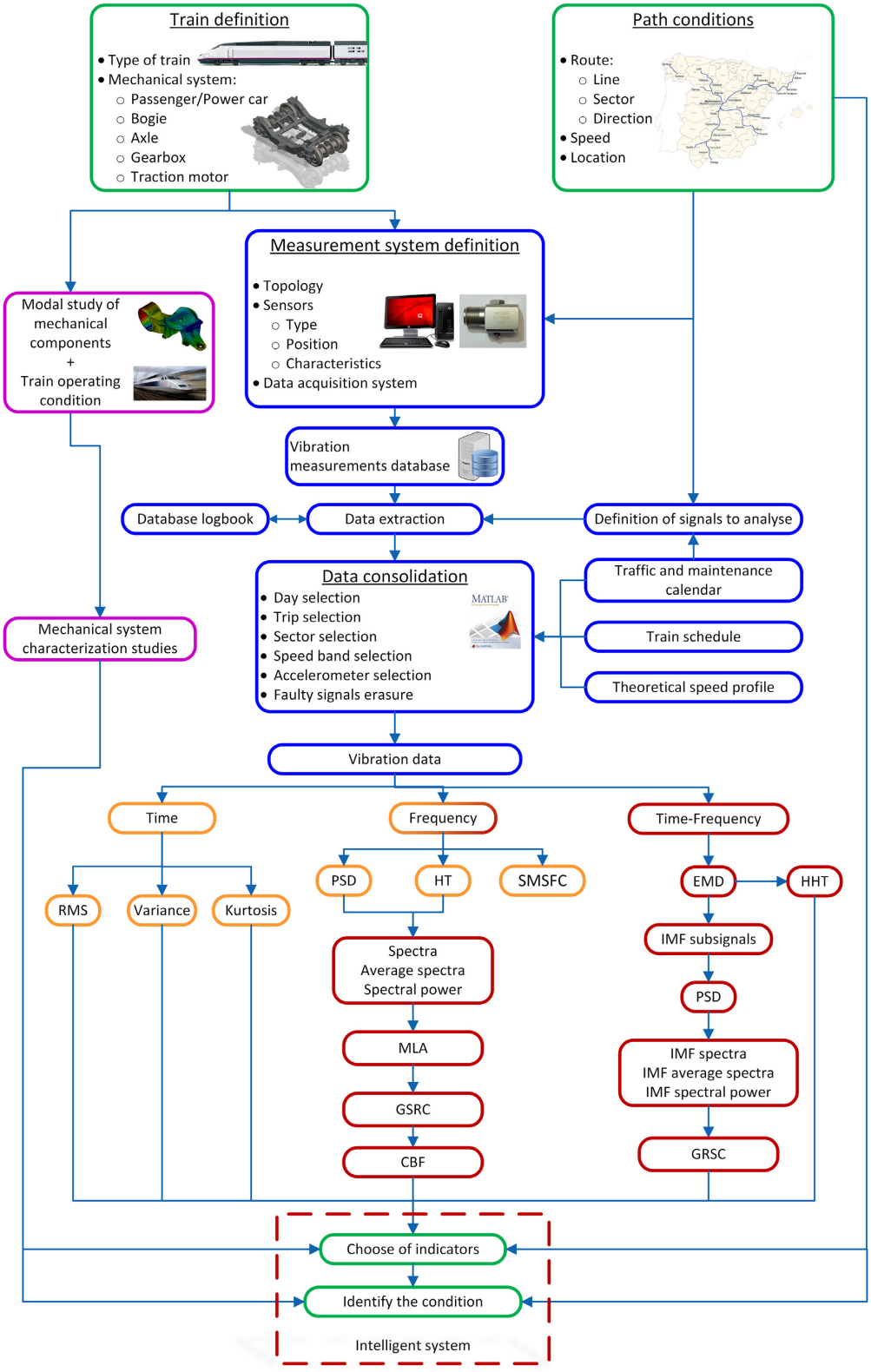

Figure 2: Algorithm flowchart.

Within the train, the mechanical system or systems to study must be defined too. A train has a lot of systems (car body, bogie, axle, gearbox, pantograph, engine and/or electric motor, air conditioning, doors, etc.) and each system has its particular characteristics. The motion and forces that act over an axle or a pantograph are completely different, and these features will determine the measurement equipment to install.

In this paper, the type of train chosen is a high-speed train (Renfe class 100). These trains started their commercial life in 1992, can reach 300 km/h, and have served on almost all

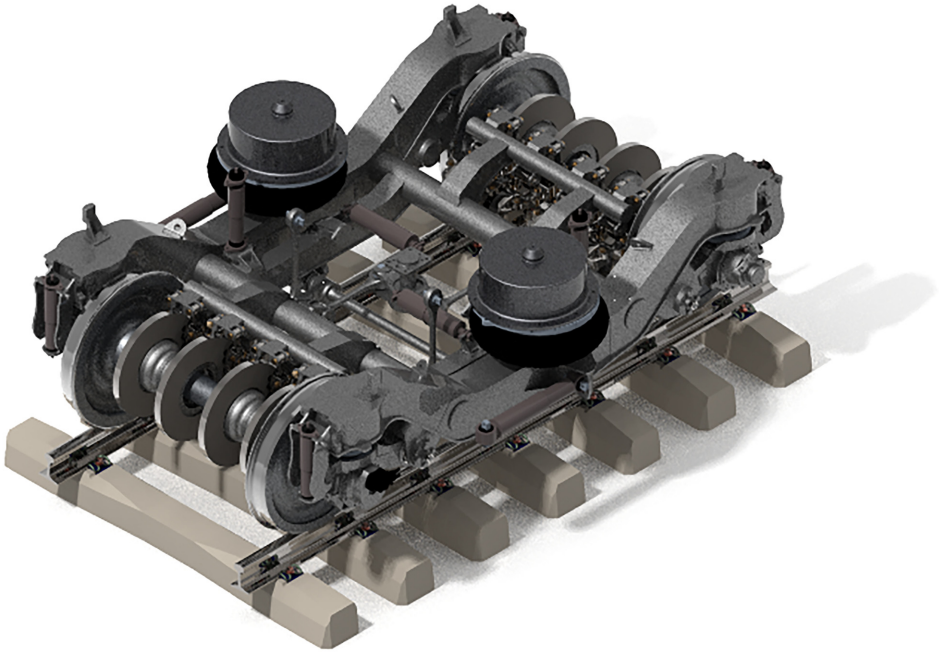

Figure 3: 3D model of the Y237B bogie.

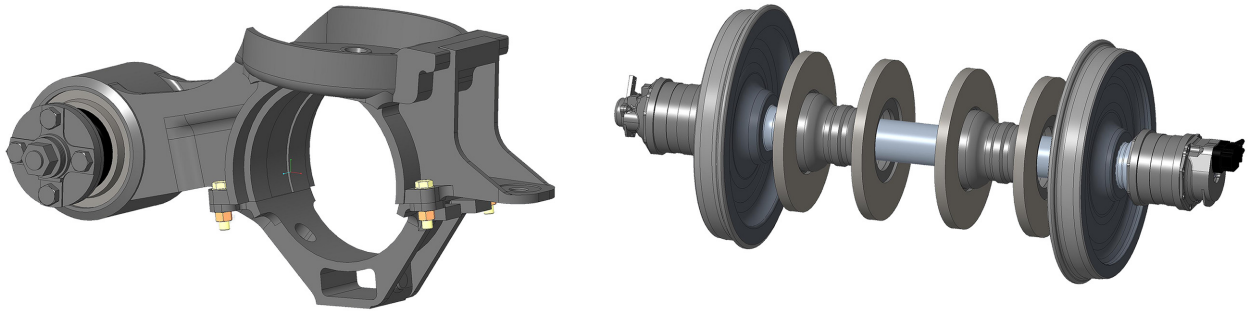

Figure 4: Detail of the axle box (left) and the wheelset (right) assemblies.

Spanish high-speed lines (HSLs). A train set is composed of two power cars at both ends and eight articulated passenger cars with Jacobs bogies. The mechanical system to study is the nearest trailer bogie to the second power car.

Track and path conditions. The track has a great influence on the performance of rail vehicles, so its main characteristics should be known. A ballast bed supports concrete sleepers that are placed every 60 cm. A rail pad is placed between the rail and the sleeper to absorb impacts and protect the sleeper. The rails are fixed to the sleepers through rail clips.

In order to take vibration measures in similar conditions, the train must run at a consistent speed. Usually, this condition is achieved on top speed sections. Besides, the section must be long enough to get an adequate number of vibration measures, and it must be easily identifiable from the available data. By taking into account these requirements, two study sections are proposed: one on the Madrid–Seville HSL and one on the Madrid–Alicante HSL.

The selected sections for recording vibration data are between 100 and 150 km long and correspond to the maximum track speeds: 270 km/h in the Madrid–Seville HSL and 300 km/h in the Madrid–Alicante HSL.

2.2.2. *Digital twin*

The digital twin is generated to perform the characterization of the mechanical system and to develop upgrades if needed. As explained earlier, the digital twin is a virtual representation of a physical system that can reproduce the behaviour of the actual system. To achieve this purpose, the digital twin may be composed of several models. The digital twin used in this work consists of a 3D model, analytical expressions for computing interesting frequencies of some subsystems, and numerical models.

Mechanical system characterization. A detailed 3D model of the bogie is designed in CREO Parametric (see Fig. 3) according to technical information provided by the manufacturer. The bogie frame, wheelsets, axle boxes, primary and secondary suspensions, bogie–car joints, and brake system are modelled in an extremely detailed way (see Fig. 4). Hence, the interaction between the more than 780 parts that made up the bogie can be

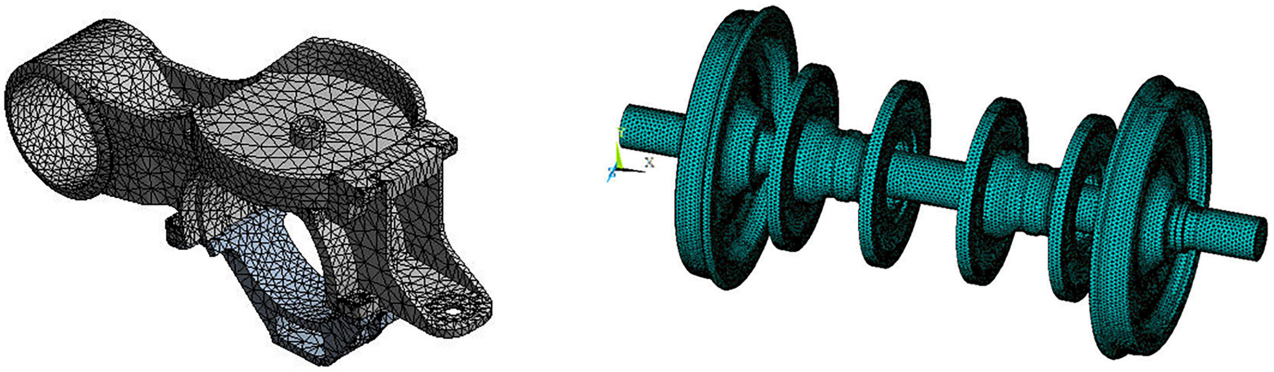

Figure 5: FEM model of the axle box (left) and the wheelset (right).

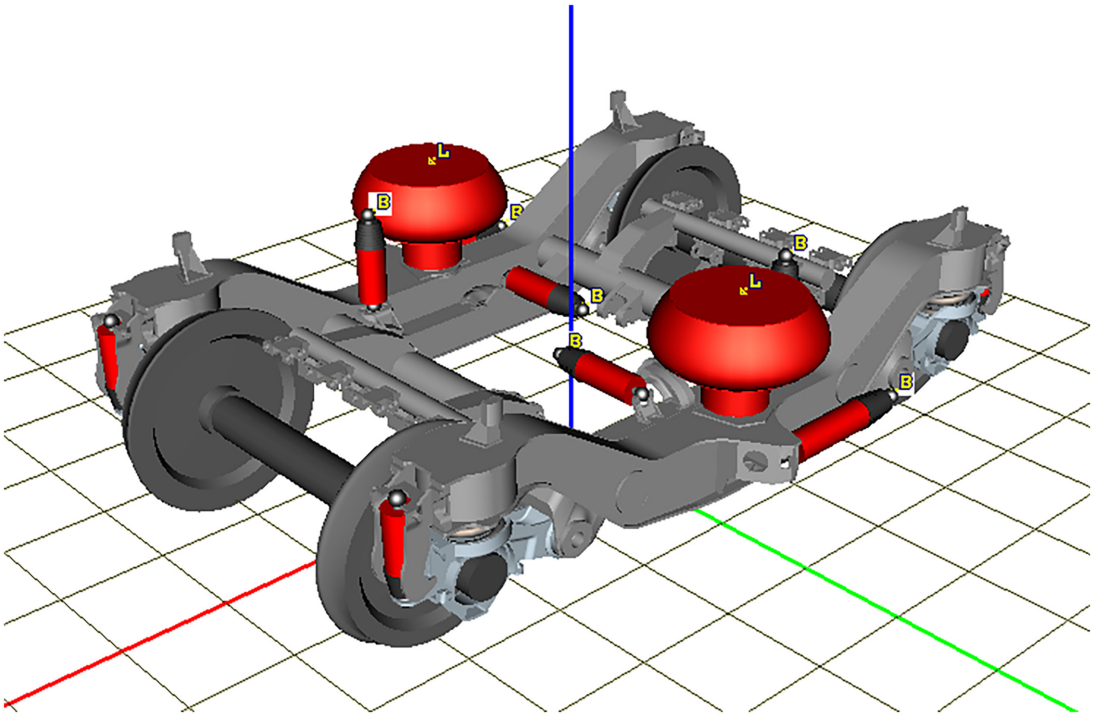

Figure 6: The multibody digital twin of the Y237B bogie in Universal Mechanism.

studied. Besides, this model can be the start point for implementing augmented reality in maintenance tasks.

Key parts of the bogie are imported in FEM software so that modal analyses can be carried out (see Fig. 5). Thanks to these modal analyses, the natural frequencies of the mechanical elements (alone or in combination with others) are obtained.

Multibody software Universal Mechanism is used for creating a multibody model of the bogie (see Fig. 6), which consists only of rigid bodies. This software is specially designed for simulating rail vehicles and allows achieving a better understanding of the train's performance under different conditions.

The other pillar of the digital twin is the computation of the characteristic frequencies of the system that cannot be obtained directly from the virtual models but depend on the speed of the train, i.e. axle rotating frequency, bearing fault frequencies, sleeper pass frequencies, etc.

Roller bearing fault frequencies (Palmgren & Ruley, 1959) are computed in equations (1)–(4), where BPFI, BPFO, BSF, and FTF are the Ball Pass Frequency Inner race, Ball Pass Frequency Outer race, Ball Spin Frequency, and Fundamental Train Frequency, respectively.

$$\mathrm{BPFI} = \frac{N_b}{2} F_s \left(1 + \frac{d}{D} \cos\beta\right) \tag{1}$$

$$\mathrm{BPFO} = \frac{N_b}{2} F_s \left(1 - \frac{d}{D} \cos\beta\right) \tag{2}$$

$$\mathrm{BSF} = \frac{D}{2d} F_s \left[1 - \left(\frac{d}{D}\right)^2 \cos^2\beta\right] \tag{3}$$

$$\mathrm{FTF} = \frac{F_s}{2} \left(1 - \frac{d}{D} \cos\beta\right) \tag{4}$$

N_b is the number of rolling elements, F_s is the axle rotating frequency, D is the average diameter of the bearing, d is the diameter of the rolling element, and β is the contact angle.

The sleeper pass frequency (SPF) is computed using equation (5), where v is the speed of the train in m/s and λ is the distance

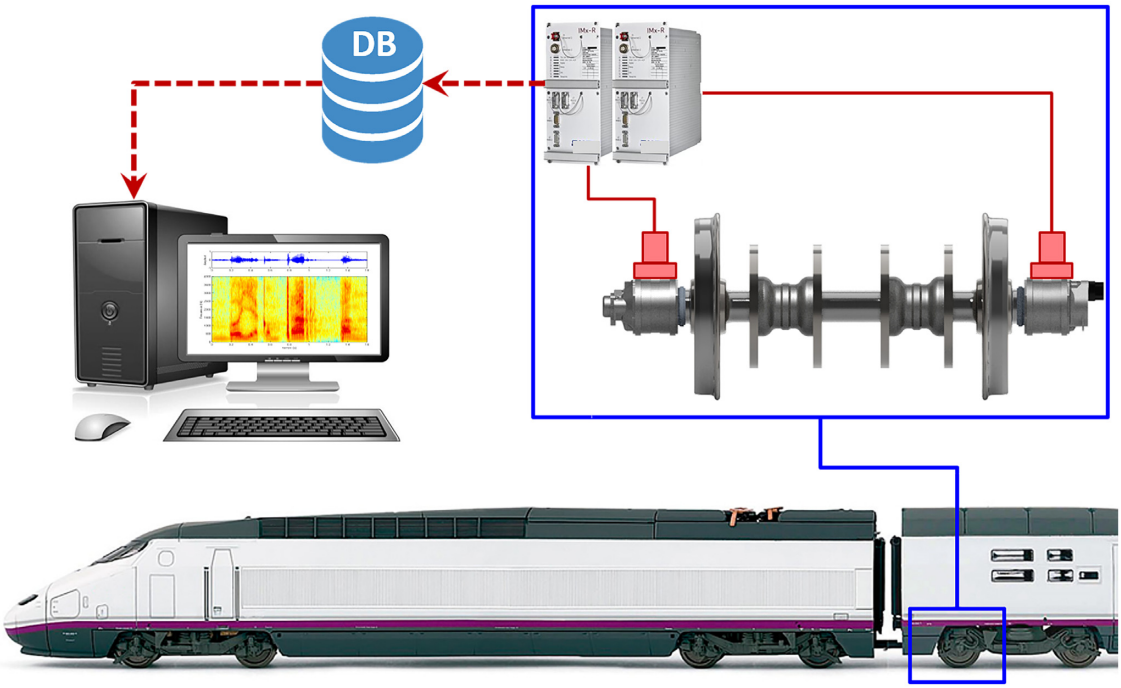

Figure 7: Scheme of the ICT infrastructure.

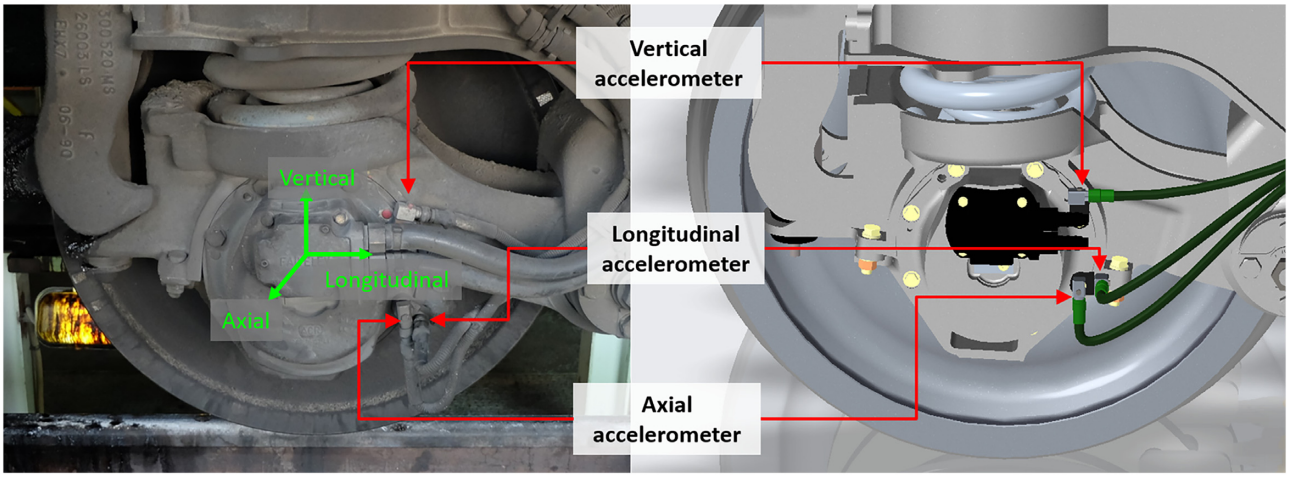

Figure 8: Location of the accelerometers. Left: real vehicle. Right: digital twin.

between sleepers.

$$\mathrm{SPF} = \frac{v}{\lambda} \tag{5}$$

2.2.3. *ICT infrastructure*

The ICT infrastructure is composed of the onboard measurement system, the storage system, and all the required tasks for the management of the data.

Onboard measurement system. The measurement equipment should be chosen according to the characteristics of the mechanical system and the track or path conditions. This equipment consists of several sensors, the signal acquisition system, and the transmission system. Vibration measures are taken from the nearest trailer axle to the second power car, as it is shown in Fig. 7.

Six uniaxial accelerometers and a speed sensor are installed on the axle, specifically, in both axle box covers. The location of the sensors is shown in Fig. 8. ICP industrial use accelerometers and speed sensors are provided by SKF®. Accelerometers are model CMSS-RAIL-9100, whose performance characteristics are shown in Table 1. The speed sensor is an Axletronic® embedded in the left axle box.

In addition to the sensors, the following technical equipment is located inside the car: a power supply, a UMTS (3G) router, and two IMx-R units. IMx-R units are provided by SKF® for data acquisition and pre-processing. Each IMx-R is equipped with 20 analogical and 4 digital input channels and can adjust the gain automatically. The system is capable of measuring and sending the speed signal one time per second and up to four vibration signals per accelerometer and minute.

Table 1: Accelerometer characteristics.

Parameter	Value
Sensitivity (±20%)	10.2 mV/(m/s^2)
Acceleration range	±490 m/s^2
Frequency range (±3dB)	0.52 Hz to 8 kHz
Resonance frequency	25 kHz
Amplitude linearity	±1%
Transverse sensitivity	≤7%

Table 2: Signal acquisition parameters.

Parameter	Value
Sampling frequency (Fs)	5120 Hz
Acquisition time (per signal)	3.2 s
Number of points *N* (per signal)	16 384 (2^{14})
Angular speed range for acquisition	75–2000 rpm
Linear speed range for acquisition	13–347 km/h

The 3G router is in charge of the communication between the onboard measurement system and the storage system. Measured data are sent to the remote database by using cell phone networks.

The system is configured to acquire data with the parameters shown in Table 2.

Storage system. Thousands of data can be recorded in one single journey, so a storage system able to manage big data is mandatory. The key part of the storage system is a computer connected to the internet that has installed the @ptitude Observer suite. This software suite is responsible for the communication server and data storage. The server software manages the incoming connections (from the 3G router aboard the train) and the data transfer. Then, these data are stored in a database. Specifically, the database saves the speed and vibration signals and, also, information about the measure as the date and the accelerometer.

Data management. Data stored in the database must be converted to MATLAB before analysing them. This task is carried out by executing a MATLAB routine that selects and extracts the data from the database and generates a MATLAB file that contains the vibration signal, the rotating speed of the wheel, and other useful information for each database record.

If the intended diagnosis is short term, the data management process ends here. However, if the intended diagnosis is long term or focused on specific dates or events, data management requires a more careful process.

In this case, the management process requires the use of several public and private documents that help to trace the train in the HSL and that contain information about the daily occurrences. By combining these documents, it is possible to select specific days, HSL sectors, and known conditions of the train to perform the long-term diagnosis. Once the data to analyse are chosen, the next step is to execute the MATLAB routine to convert data and dismiss faulty signals (if they exist) before proceeding to the analysis.

2.2.4. *Diagnosis*

In this last step, the signal analysis is performed. Several signal processing techniques in time, frequency, and time–frequency domains are used for this task. All these techniques are explained in detail in the next section.

The analysis of the vibration data allows selecting a group of parameters or indicators that represent the condition of the studied mechanical system.

Although all the signal processing techniques can offer valuable information about the status of the mechanical system, their computation time makes them more suitable for short-term diagnosis or long-term diagnosis. Methods like RMS (root mean square), variance, kurtosis, PSD (power spectral density), HT (Hilbert Transform), or SMSFC (Selection of the Most Significant Frequency Components) require short computation time and can be applied almost in real time. The other techniques take longer computation times, so they are suitable for long-term diagnosis.

3. Signal Processing Techniques

As exposed earlier, the vibration signals are processed by using techniques in time, frequency, and time-domain analyses that can be classified into short-term diagnosis or long-term diagnosis.

This section depicts the techniques mentioned in the algorithm flowchart briefly.

3.1. Short term

3.1.1. *Time-domain analysis*

Four statistical parameters are selected for the time-domain analysis: average, RMS, variance, and kurtosis. Although these parameters do not offer a detailed analysis of the signal, they can give an overview of the system's status. These parameters are basic concepts of statistics and are well described in any statistics book, so we will not describe them here.

3.1.2. *Frequency-domain analysis*

A combination of both classical and novel techniques is selected for the frequency-domain analysis. Taking the PSD and the envelope spectrum as a foundation, a set of new techniques is developed.

The PSD can be computed from the Fourier transform by using equation (6), where Δt is the sample time, N is the number of data points in the signal, and $X(f)$ is the Fourier transform of the signal.

$$\mathrm{PSD} = \mathrm{S}(f) = \frac{\Delta t}{N}\left|X(f)\right|^2 \tag{6}$$

The envelope spectrum is another well-known technique that computes the PSD from the HT of the signal. The HT is a useful mathematical tool for describing the complex envelope of a signal modulated by an actual carrier signal. The HT of a signal is another (time) signal defined by equation (7).

$$H\left[x(t)\right] = \hat{x}(t) = \frac{1}{\pi}\int_{-\infty}^{\infty}\frac{x(\tau)}{t-\tau}\mathrm{d}\tau = x(t)\otimes(1/\pi t) \tag{7}$$

The envelope spectrum is useful to amplify low-frequency modulations and is also a powerful tool for detecting faults in roller bearings.

The SMSFC is an own-developed method for detecting and counting the number of highest peaks of the spectra. The developed algorithm locates the most significant frequency components (highest peaks) of each analysed signal and orders them from highest to lowest. Then, the algorithm rounds the frequency of each peak to the nearest integer. Next, it counts the '*n*'

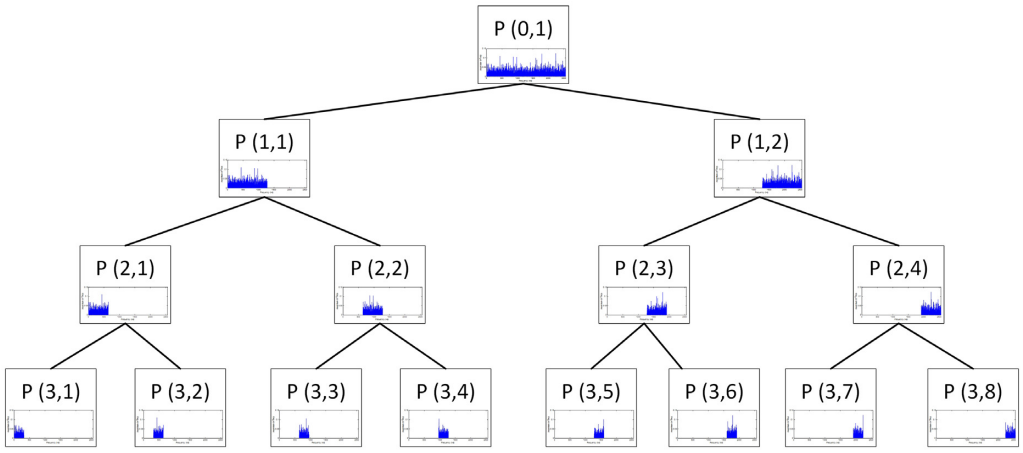

Figure 9: Scheme of the decomposition process of MLA.

peaks in all the signals of the section to be analysed. The value '*n*' is arbitrary and can be established according to the study objectives.

In addition to SMSFC, an algorithm for automatic detection of non-harmonics is developed. This algorithm identifies the frequency components that do not match a multiplier or harmonic of the axle rotating frequency and highlights them with a red circle. The precision of the multipliers and the minimum relative energy of the frequency components can be adjusted as required.

3.2. Long term

3.2.1. *Frequency-domain analysis*

The spectra (from the PSD or PSD of the HT) can be decomposed into frequency bands or packets. This process is known as Multi-Level Analysis (MLA). MLA splits the spectrum into two halves, each of which can be split again into two halves, and so on. At each level, 2^k packets are obtained, k being the decomposition level. Figure 9 shows the decomposition process of any signal spectrum.

Every frequency band or packet will have a different power. The power of a packet (k, j) is given by equation (8), where i is the index of the signal array, j is the packet number for a decomposition level k ($1–2^k$), k is the decomposition level, N is the number of points of the signal, $S_x(i)$ is the value of the PSD at index i, and $P(k, j)$ is the power of the packet j for the decomposition level k.

$$P(k,\ j) = \sum_{j=1}^{j=2^k} \sum_{i=\frac{N}{2^k}(j-1)+1}^{i=\frac{N}{2^k}j} S_x(i) \tag{8}$$

The Graphical Representation of State Configurations (GRSC) technique is based on the MLA. Vibration signals are recorded before and after a significant event (for example, a maintenance action or a failure) and grouped into three operating states. PSD and MLA are applied to every signal. Then, the average spectral power for each group (state) and each frequency band is computed. These spectral powers are plotted in a time–power graph and linked with lines, so a triangle is obtained. This triangle represents the state of the mechanical system. According to the configuration of the states (the triangle's shapes), it can be established the power evolution of a certain frequency band. A detailed explanation of this method can be found in Bustos *et al.* (2019, 2021).

The Chromogram of Bands of Frequency (CBF) method is based on the GRSC. This technique assigns a colour code to the configuration states of the GRSC. Then, a colour map is built in a frequency-decomposition level axis. Therefore, the evolution of the spectral power of a given frequency band is easily recognizable and information about the state of the mechanical system can be retrieved with just a glance on the CBF. This technique is described in detail in Bustos *et al.* (2019, 2021).

3.2.2. *Time–frequency-domain analysis*

The Empirical Mode Decomposition (EMD) and the Hilbert–Huang Transform (HHT) were first proposed by Huang *et al.* (1998). The EMD can decompose a signal into a set of subsignals called Intrinsic Mode Functions (IMFs). The decomposition algorithm is well documented in the literature (Huang *et al.*, 1998; Rilling *et al.*, 2007).

The HHT applies the HT to obtained IMF and computes the instant frequencies too. That way, the relationship between the time, the frequency, and the amplitude can be plotted in a graph.

4. Results

The methodology explained in Sections 2 and 3 is tested using actual vibration signals recorded from a Renfe class 100 high-speed train in normal operating conditions. That is, the train is running at speeds between 270 and 300 km/h. The vibration signals are recorded in the three spatial directions and processed using the techniques mentioned earlier.

4.1. Digital twin

The numerical models of the digital twin allow computing the characteristics frequencies shown in Table 3. As the wheel radius varies due to the wheel wear, these values are calculated for the new wheel and wear limit radius at the speeds of 270 and 300 km/h. Therefore, a value range is given in all frequencies that depend on the wheel radius or the axle rotating frequency.

The characteristic frequencies of the track are obtained from the literature (Thompson, 2009; Connolly *et al.*, 2015; Zougari *et al.*, 2016) and summarized in Table 4, as the wheel corrugation frequency or the track resonance frequencies.

The numerical (FEM) model of the digital twin is used to compute the free natural frequencies of key parts of the bogie. The parts are meshed using solid elements with 10 nodes. The size

Table 3: Train characteristic frequencies at 270 and 300 km/h for new and worn wheels.

Phenomenon	Frequency (Hz) at 270 km/h	Frequency (Hz) at 300 km/h
Axle rotating frequency (F_r)	25.95–28.09	28.83–31.21
Ball Pass Frequency Inner Race (BPFI)	329.14–356.24	365.71–395.83
Ball Pass Frequency Outer Race (BPFO)	267.69–289.74	297.44–321.93
Ball Spin Frequency (BSF)	122.84–132.96	136.49–147.73
Fundamental Train Frequency (FTF)	11.65–12.61	12.95–14.01
Wheel corrugation frequency	1500–3500	
Primary suspension – wheelset frequency/wheelset bounce	~2.5–3	

Table 4: Track characteristic frequencies at 270 and 300 km/h.

Phenomenon	Frequency (Hz) at 270 km/h	Frequency (Hz) at 300 km/h
SPF	125	138.89
Rail/sleeper–ballast resonance	40–300	
Rail–rail pad resonance	200–600	
Rail pinned–pinned resonance	~1000	

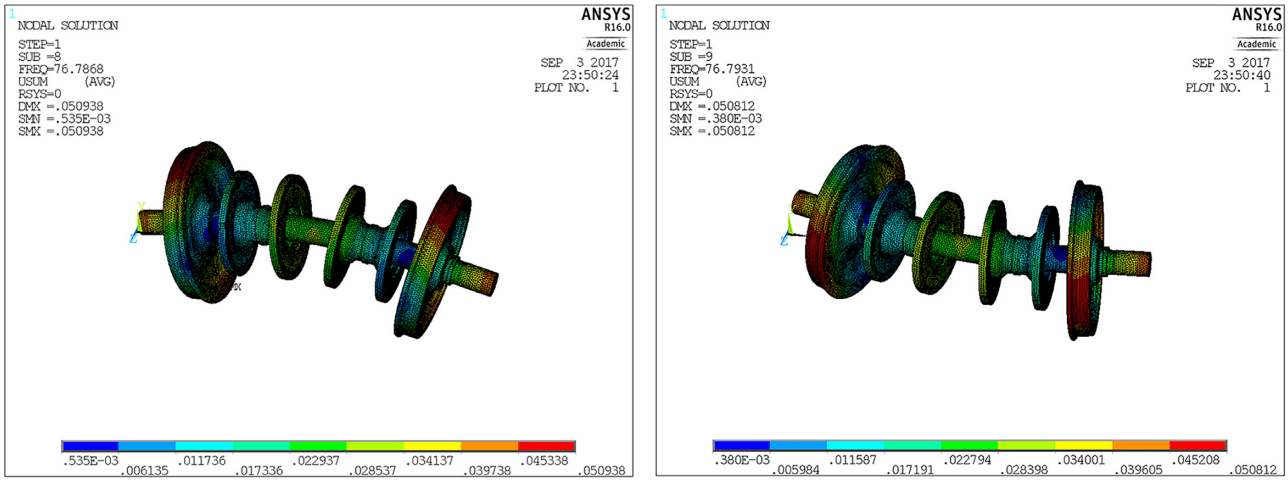

Figure 10: Natural modes of the wheelset.

of the elements is chosen according to the geometry of the part, so it is defined properly without excessive computation requirements.

The FEM modelled parts are the bogie frame, the wheelset, the two-piece axle box, the upper and lower pieces of the axle box, the bearing housing, the axle box covers, and the rings of the roller bearing.

The natural modes of the wheelset are obtained by considering it as one component and considering its parts (axle, wheel, and brake discs) separately. Representative natural modes of the wheelset and the axle box are chosen to illustrate the results of the numerical modal analysis. Figure 10 shows the first bending mode of the wheelset, which occurs in the vertical and horizontal planes at a frequency of 76.7 Hz. The first two natural vibration modes of the axle box occur at 410 and 480 Hz. The first is a bending mode, whereas the latter is a torsion mode, as can be seen in Fig. 11.

4.2. Diagnosis

This subsection displays the typical graphical results that can be obtained from the application of the SMSFC, GRSC, CBF, and EMD techniques. The results shown in the following pages are the product of applying these signal processing techniques to actual vibration measurements recorded during the train operation. Vibration signals were recorded at an average speed of 270 km/h in the Madrid–Seville HSL in three different operating conditions: before a maintenance action, just after this maintenance operation, and some weeks later.

Figure 12 shows the typical image that can be obtained from the application of the SMSFC method. This image is composed of three plots that represent the signal waveform, the PSD of the signal, and the normalized PSD of the signal highlighting the non-harmonic components with a red circle. The minimum relative energy of 5% highest peak is set to generate Fig. 12.

As it can be observed, there are three main active areas on the spectrum: between 0 and 350 Hz, between 500 and 1000 Hz, and between 1500 and 2560 Hz.

To get a clearer view of the frequency components highlighted by the SMSFC algorithm, the frequency region between 0 and 800 Hz is presented in Fig. 13. The highest amplitude frequency components are located at 124.1 and 270 Hz, which correspond to 4.73 and 10.3 times the axle rotating frequency, respectively. Consequently, they are highlighted in the last plot of

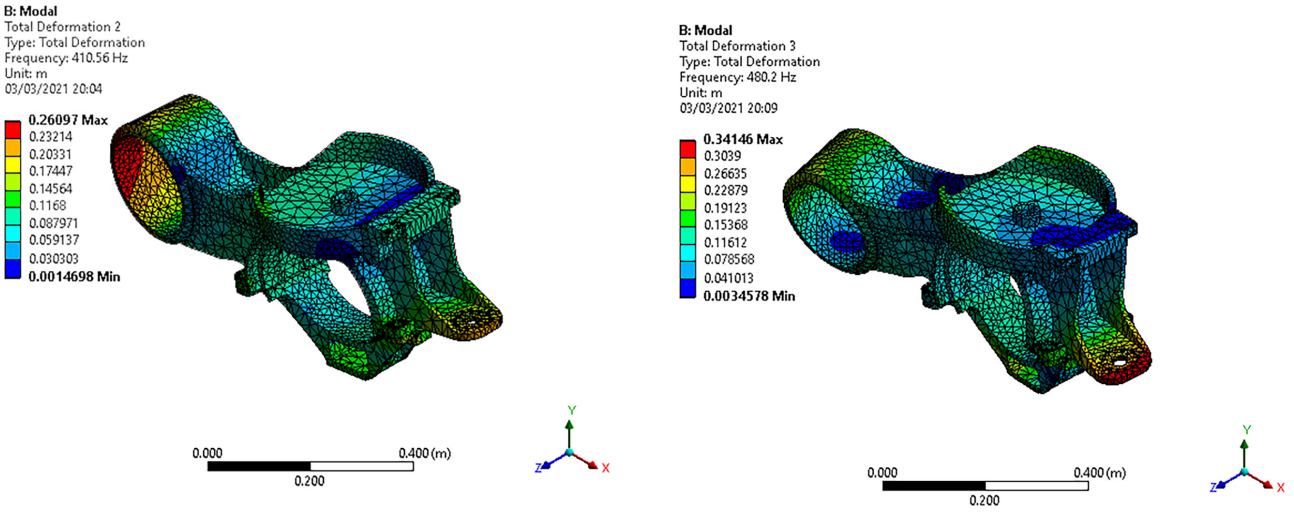

Figure 11: Natural modes of the axle box assembly.

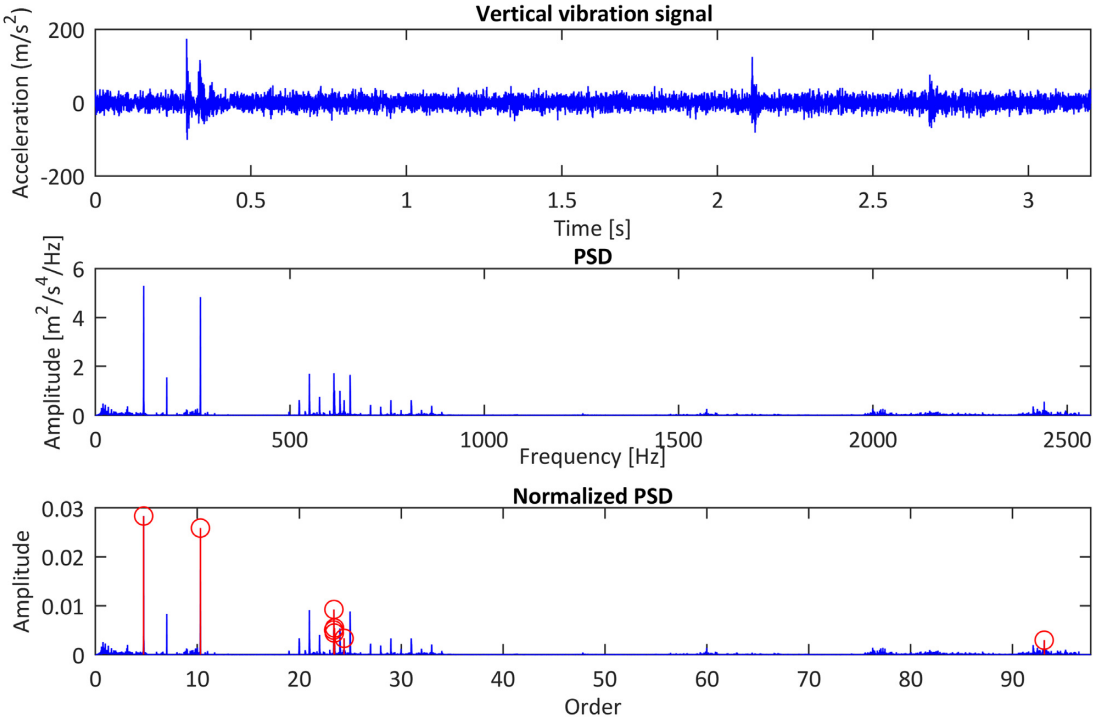

Figure 12: Signal waveform, PSD, and non-harmonic components of an actual vertical vibration signal that was recorded at 270 km/h.

the figure. These frequencies match the SPF (speed is slightly below 270 km/h) and the BPFO of the rolling bearing. The significant frequency component located between the previous two corresponds to the seventh harmonic of the axle rotating frequency.

Between 500 and 1000 Hz, there are lots of components that are multipliers of the axle rotating frequency mainly. However, the SMSFC detects frequency components at 23.4 and 24.4 times the rotating frequency of the axle. The high-frequency region is mainly related to the wheel corrugation phenomenon (Connolly *et al.*, 2015) and only a small non-harmonic component is detected by the SMSFC.

An example of the GRSC is shown in Fig. 14. Results are presented up to decomposition level 2, but the decomposition level can be increased up to 9, which would produce 1023 different configurations (triangles).

The results showed here correspond to vibration measurements taken before (operating state B), just after (operating state A), and some weeks after (operating state L) wheel reprofiling. The spectral power of the signals recorded in each operating state is averaged and displayed as points in the image. The name of the configuration is created by looking at the straights that join the points of the operating states. It is a three-letter structure ('xxx') in which the first letter corresponds to the red line

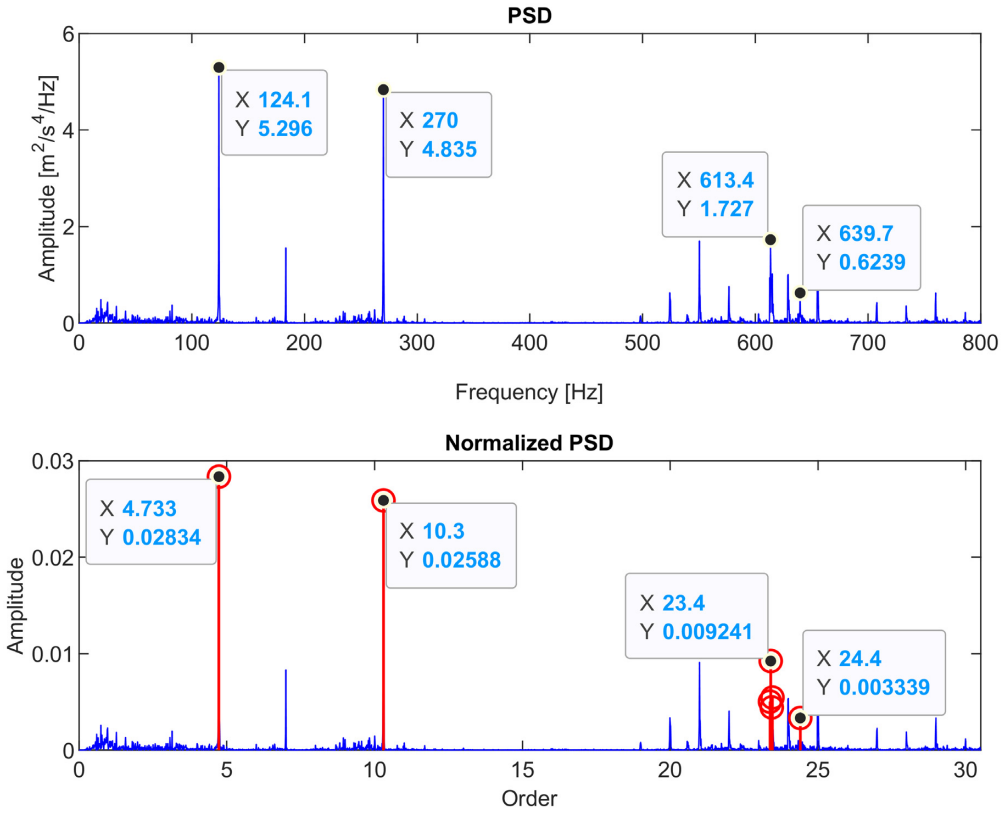

Figure 13: Details of the PSD and non-harmonic components of Fig. 12 in the region 0–800 Hz.

(B→A), the second letter corresponds to the green line (A→L), and the third letter corresponds to the blue line (B→L). The value of each position can be 'd' (down, for negative slopes) or 'u' (up, for positive slopes).

The upper plot of Fig. 14 belongs to decomposition level $k = 0$ and shows the time evolution of the spectral power of the vibration signals. This power is reduced just after the maintenance action, as it should be expected. Besides, the power is also reduced in the following weeks after the wheel reprofiling. Therefore, the configuration is 'ddd' as the spectral power is reduced between two states always.

Decomposition level $k = 1$ divides the spectrum into two. In the low-frequency region, the power rises just after the wheel reprofiling, but it is lower at the end of the analysed period. As the power rises between operating states B and A, and falls between A and L, and between B and L, the configuration is 'udd'. Regarding the high-frequency region, the spectral power decreases always after the wheel reprofiling. Hence, the configuration is 'ddd'.

Decomposition level $k = 2$ splits the spectrum into four parts or power packets. The first, third, and fourth packets have the same behaviour of $k = 0$ and the spectral power is always reduced. However, the spectral power of the second packet rises just after the wheel reprofiling and then decreases, although the spectral power at the end of the studied period is greater than the power before the wheel reprofiling.

The CBF compiles the information of decomposition levels from $k = 0$ to 9 in one image and is shown in Fig. 15. The first row of the CBF corresponds to decomposition level $k = 0$ and matches the 'ddd' configuration of GRSC, so it is coloured in dark blue according to the colour palette of Bustos *et al.* (2019). The second row relates to decomposition level $k = 1$, and we find two colours that correspond to the two GRSC configurations. The same procedure is applied for the rest of the rows.

The CBF can be divided into two halves. The right half (between 1280 and 2560 Hz) is mainly coloured in blue, which is the expected performance of the system after a maintenance work (spectral power or vibration is reduced after maintenance). Just small red and orange stripes appear at high decomposition levels around 1750 Hz.

The left half (0–1280 Hz) shows a different image: A large bandwidth that spreads from 600 to 1300 Hz is coloured in warm colours. This indicates that the spectral power is increased just after the maintenance operation. Cold colours are the prevailing colours between 0 and 600 Hz, although some orange stripes are also visible.

The application of the EMD technique to the signal of Fig. 12 results in the graph of Fig. 16. The first six IMFs are extracted and, then, the PSD of each IMF is computed and plotted in the same figure. By comparing the frequency regions mentioned earlier and the results of the EMD, it can be observed that IMF (1) matches the high-frequency region (1500–2560 Hz), the second and third IMFs correspond to the 500–1000 Hz region, and that the low-frequency region is composed of IMFs (4), (5), and (6).

It should also be noted that the SPF and BPFO components are assigned to different IMFs, which is consistent with different physical origins (Bustos *et al.*, 2018).

4.3. Intelligent system

The operating condition of the mechanical system (a high-speed train in this example) can be identified based on the previous

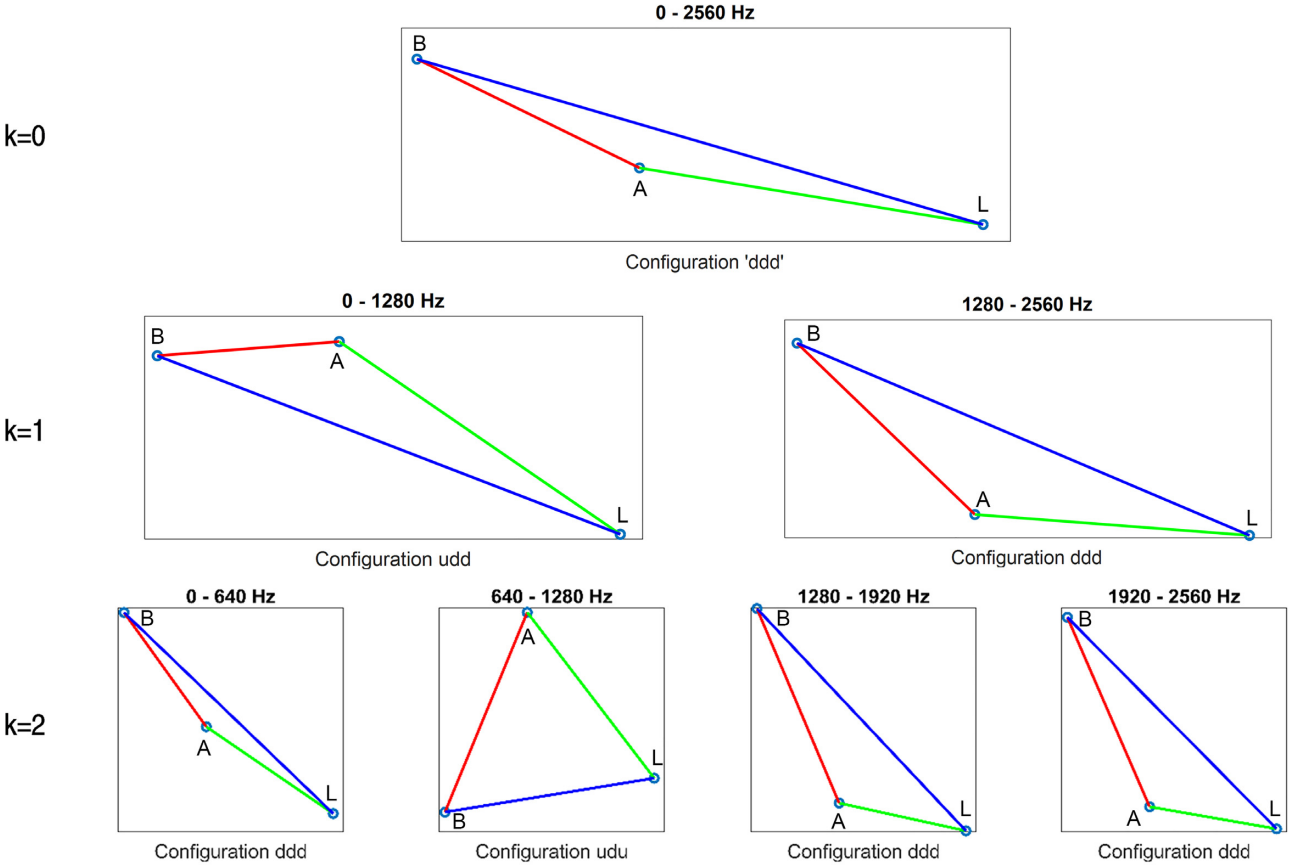

Figure 14: GRSC of actual vertical vibration signals recorded at 270 km/h.

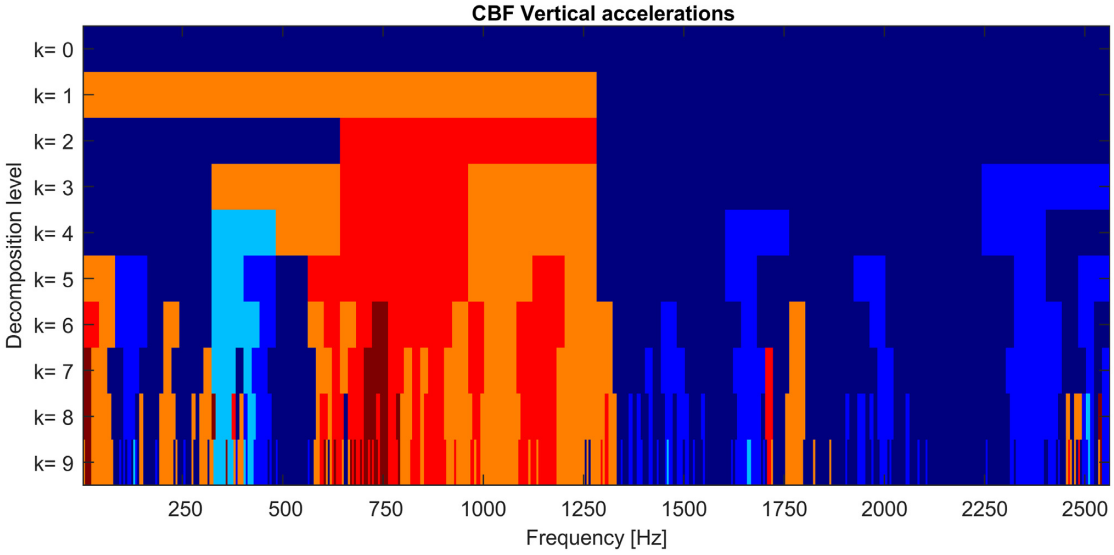

Figure 15: CBF of actual vertical vibration signals recorded at 270 km/h.

results. However, this task requires the correct interpretation of the data by expert personnel.

However, within the Industry 4.0 paradigm is more suitable to use an intelligent system to do this task. Once trained, this intelligent system will be able to identify the operational condition of the system from the results of the signal processing techniques explained in Section 2 without any kind of human intervention.

The inputs of this intelligent system will be a set of indicators obtained from the quantification of the results shown in the previous subsection (for example, the power of the packets, spectral power of the IMFs, etc.). Besides, the system characteristics

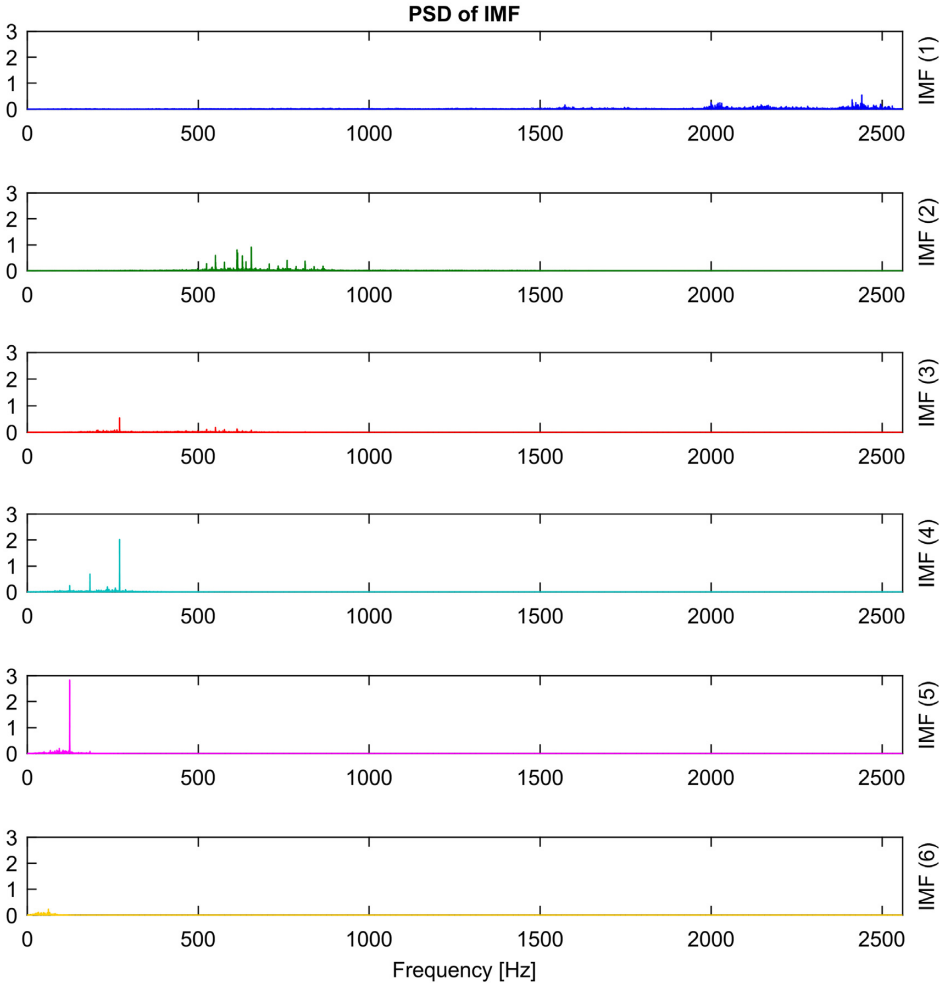

Figure 16: Power spectra of the first six IMFs of an actual vertical vibration signal recorded at 270 km/h. Values of the vertical axis are expressed in $(m^2/s^4)/Hz$.

obtained through the digital twin would be used to label the identifiers and thus train the intelligent system.

5. Conclusions

This paper presents a methodology for retrofitting and updating to Industry 4.0 a high-speed train designed and manufactured before the development of Industry 4.0. The proposed methodology is mainly focused on Maintenance 4.0, but it also makes use of other modern concepts such as digital twin, big data, or artificial intelligence, and it is ready to use augmented reality.

In this manuscript, all aspects of the proposed methodology are explained in detail, as well as the characteristics that data acquisition (including sensors) and communication infrastructure must satisfy. Also, the signal processing techniques for analysing vibration data are described, including new own methods (SMSFC, GRSC, and CBF) that are developed within this methodology. The selected signal processing techniques allow analysing experimental data both in real time and deferred, according to the maintenance or user requirements.

The proposed methodology is applied to a Spanish high-speed train during its normal operation, recording vibration data from the axle boxes of a trailer bogie for several years. Vibration data are collected and processed in designated sections of the track where the train reaches its maximum speed, as this is the most critical condition. The digital twin of the bogie is built based on four pillars: a detailed 3D model, FEM models of key parts, a multibody model, and the computation of theoretical characteristic frequencies

The digital twin allows obtaining the natural and characteristic frequencies of the system in different conditions. On the other hand, from the vibration measurement processing, several graphs are obtained, which allows analysing the operating state of the train. By combining both results, it is possible to establish what frequencies correspond to the normal running of the train and what frequencies could correspond to anomalies in the train performance. These frequencies will be the input indicators for the intelligence system, which should be able to identify the train condition on its own.

Specifically, SMSFC allows focusing on high-amplitude frequency components that are not multipliers of the axle rotating frequency, like those located at 124.1 and 270 Hz, which correspond to 4.73 and 10.3 times the axle rotating frequency, respectively. The first one corresponds to the SPF, while the latter matches the BPFO of the rolling bearing.

The use of long-term signal processing techniques GRSC and CBF for studying the performance of the high-speed train before and after a maintenance operation confirms that high frequencies are excited by phenomena like wheel corrugation, and they are reduced when the wheel corrugation is eliminated.

List of Acronyms

BPFI:	Ball Pass Frequency Inner race
BPFO:	Ball Pass Frequency Outer race
BSF:	Ball Spin Frequency
CBF:	Chromogram of Bands of Frequency
CBM:	Condition-Based Maintenance
CMM:	Coordinate Measuring Machines
EMD:	Empirical Mode Decomposition
FEM:	Finite Element Method
FTF:	Fundamental Train Frequency
GRSC:	Graphical Representation of State Configurations
HHT:	Hilbert–Huang Transform
HSL:	High-Speed Line
HT:	Hilbert Transform
ICP:	Integrated Circuit Piezoelectric
ICT:	Information and Communication Technology
IMF:	Intrinsic Mode Function
MLA:	Multi-Level Analysis
PSD:	Power Spectral Density
RMS:	Root Mean Square
SMSFC:	Selection of the Most Significant Frequency Components
SPF:	Sleeper Pass Frequency
SQL:	Structured Query Language
UMTS:	Universal Mobile Telecommunications System

Acknowledgements

The research work described in this paper was supported by the Spanish Government through the MM-IA4.0 PID2020-116984RB-C21 and RMS4.0 PID2020-116984RB-C22 projects.

Conflict of interest statement

None declared.

References

Alemi, A., Corman, F., & Lodewijks, G. (2017). Condition monitoring approaches for the detection of railway wheel defects. *Proceedings of the Institution of Mechanical Engineers, Part F: Journal of Rail and Rapid Transit*, *231*(8), 961–981. https://doi.org/10.1177/0954409716656218.

Alstom. (2014, September 24). *Alstom launches HealthHub, an innovative tool for predictive maintenance*. Global Railway Review. https://www.globalrailwayreview.com/news/21579/alstom-launches-healthhub-an-innovative-tool-for-predictive-maintenance/.

Amini, A., Entezami, M., Huang, Z., Rowshandel, H., & Papaelias, M. (2016). Wayside detection of faults in railway axle bearings using time spectral kurtosis analysis on high-frequency acoustic emission signals. *Advances in Mechanical Engineering*, *8*(11), 1–9. https://doi.org/10.1177/1687814016676000.

Bernal, E., Spiryagin, M., & Cole, C. (2019). Onboard condition monitoring sensors, systems and techniques for freight railway vehicles: A review. *IEEE Sensors Journal*, *19*(1), 4–24. https://doi.org/10.1109/JSEN.2018.2875160.

Bustos, A., Rubio, H., Castejon, C., & Garcia Prada, J. C. (2021). Enhancement of chromatographic spectral technique applied to a high-speed train. *Structural Control and Health Monitoring*, *28*(12), e2842. https://doi.org/10.1002/stc.2842.

Bustos, A., Rubio, H., Castejón, C., & García-Prada, J. (2018). EMD-based methodology for the identification of a high-speed train running in a gear operating state. *Sensors*, *18*(3), 793. https://doi.org/10.3390/s18030793.

Bustos, A., Rubio, H., Castejon, C., & Garcia-Prada, J. C. (2019). Condition monitoring of critical mechanical elements through graphical representation of state configurations and chromogram of bands of frequency. *Measurement*, *135*, 71–82. https://doi.org/10.1016/j.measurement.2018.11.029.

Ceruti, A., Marzocca, P., Liverani, A., & Bil, C. (2019). Maintenance in aeronautics in an Industry 4.0 context: The role of augmented reality and additive manufacturing. *Journal of Computational Design and Engineering*, *6*(4), 516–526. https://doi.org/10.1016/j.jcde.2019.02.001.

Cheng, Y.-H., & Tsao, H.-L. (2010). Rolling stock maintenance strategy selection, spares parts' estimation, and replacements' interval calculation. *International Journal of Production Economics*, *128*(1), 404–412. https://doi.org/10.1016/j.ijpe.2010.07.038.

Chong, S. Y., Lee, J.-R., & Shin, H.-J. (2010). A review of health and operation monitoring technologies for trains. *Smart Structures and Systems*, *6*(9), 1079–1105. https://doi.org/10.12989/sss.2010.6.9.1079.

Connolly, D. P., Kouroussis, G., Laghrouche, O., Ho, C. L., & Forde, M.C. (2015). Benchmarking railway vibrations – Track, vehicle, ground and building effects. *Construction and Building Materials*, *92*, 64–81. https://doi.org/10.1016/j.conbuildmat.2014.07.042.

Dwyer-Joyce, R. S., Yao, C., Lewis, R., & Brunskill, H. (2013). An ultrasonic sensor for monitoring wheel flange/rail gauge corner contact. *Proceedings of the Institution of Mechanical Engineers, Part F: Journal of Rail and Rapid Transit*, *227*(2), 188–195. https://doi.org/10.1177/0954409712460986.

Fortea, P. (2018, October 18). Using predictive maintenance to improve safety and efficiency of railways. *Global Railway Review*. https://www.globalrailwayreview.com/article/74343/predictive-maintenance-safety-efficiency/.

Geren, N., Bayramoğlu, M., & Eşme, U. (2007). Improvement of a low-cost water jet machining intensifier using reverse engineering and redesign methodology. *Journal of Engineering Design*, *18*(1), 13–37. https://doi.org/10.1080/09544820600650928.

Gómez, M. J., Castejón, C., Corral, E., & García-Prada, J. C. (2020). Railway axle condition monitoring technique based on wavelet packet transform features and support vector machines. *Sensors*, *20*(12), 3575. https://doi.org/10.3390/s20123575.

Grieves, M., & Vickers, J. (2017). Digital Twin: Mitigating unpredictable, undesirable emergent behavior in complex systems. In F.-J. Kahlen, S. Flumerfelt, & A. Alves (Eds.), *Transdisciplinary perspectives on complex systems*(pp. 85–113). Springer International Publishing. https://doi.org/10.1007/978-3-319-38756-7_4.

Hassan, M., & Bruni, S. (2018). Experimental and numerical investigation of the possibilities for the structural health monitoring of railway axles based on acceleration measurements. *Structural Health Monitoring*, *18*(3), 902–919. https://doi.org/10.1177/1475921718786427.

Huang, N. E., Shen, Z., Long, S. R., Wu, M. C., Shih, H. H., Zheng, Q., Yen, N.-C., Tung, C. C., & Liu, H. H. (1998). The empirical mode decomposition and the Hilbert spectrum for nonlinear and non-stationary time series analysis. *Proceedings of the Royal Society of London A: Mathematical, Physical and Engineering Sciences*, 454, 903–995.

Hyde, P., Ulianov, C., & Defossez, F. (2016). Development and testing of an automatic remote condition monitoring system

for train wheels. *IET Intelligent Transport Systems*, *10*(1), 32–40. https://doi.org/10.1049/iet-its.2015.0041.

In-Depth Focus: Digital Twins. (2021, April). *Global Railway Review*, *27*(02), 19.

Kans, M., Galar, D., & Thaduri, A. (2016). Maintenance 4.0 in railway transportation industry. In K. T. Koskinen, H. Kortelainen, J. Aaltonen, T. Uusitalo, K. Komonen, J. Mathew, & J. Laitinen (Eds.), *Proceedings of the 10th World Congress on Engineering Asset Management (WCEAM 2015)*(pp. 317–331). Springer International Publishing. https://doi.org/10.1007/978-3-319-27064-7_30.

Karakose, M., & Yaman, O. (2020). Complex fuzzy system based predictive maintenance approach in railways. *IEEE Transactions on Industrial Informatics*, *16*(9), 6023–6032. https://doi.org/10.1109/TII.2020.2973231.

Ke, Y., Fan, S., Zhu, W., Li, A., Liu, F., & Shi, X. (2006). Feature-based reverse modeling strategies. *Computer-Aided Design*, *38*, 485–506. https://doi.org/10.1016/j.cad.2005.12.002.

Lai, C. C., Kam, J. C. P., Leung, D. C. C., Lee, T. K. Y., Tam, A. Y. M., Ho, S. L., Tam, H. Y., & Liu, M. S. Y. (2012). Development of a fiber-optic sensing system for train vibration and train weight measurements in Hong Kong. *Journal of Sensors*, *2012*, 1–7. https://doi.org/10.1155/2012/365165.

Lasi, H., Fettke, P., Kemper, H.-G., Feld, T., & Hoffmann, M. (2014). Industry 4.0. *Business & Information Systems Engineering*, *6*(4), 239–242. https://doi.org/10.1007/s12599-014-0334-4.

Lebel, D., Soize, C., Funfschilling, C., & Perrin, G. (2019). High-speed train suspension health monitoring using computational dynamics and acceleration measurements. *Vehicle System Dynamics*, *58*, 1–22. https://doi.org/10.1080/00423114.2019.1601744.

Lederman, G., Chen, S., Garrett, J. H., Kovačević, J., Noh, H. Y., & Bielak, J. (2017). A data fusion approach for track monitoring from multiple in-service trains. *Mechanical Systems and Signal Processing*, *95*, 363–379. https://doi.org/10.1016/j.ymssp.2017.03.023.

Lee, W.-H., Lee, K.-H., Lee, J.-M., & Nam, B.-W. (2020). Registration method for maintenance-work support based on augmented-reality-model generation from drawing data. *Journal of Computational Design and Engineering*, *7*(6), 775–787. https://doi.org/10.1093/jcde/qwaa056.

Li, Z., Wei, L., Dai, H., Zeng, Y., & Wang, Y. (2012). Identification method of wheel flat based on Hilbert–Huang transform. *Journal of Traffic and Transportation Engineering*, *12*(4), 33–41.

Li, C., Luo, S., Cole, C., & Spiryagin, M. (2017a). An overview: Modern techniques for railway vehicle on-board health monitoring systems. *Vehicle System Dynamics*, *55*(7), 1045–1070. https://doi.org/10.1080/00423114.2017.1296963.

Li, Y., Zuo, M. J., Lin, J., & Liu, J. (2017b). Fault detection method for railway wheel flat using an adaptive multiscale morphological filter. *Mechanical Systems and Signal Processing*, *84*, 642–658. https://doi.org/10.1016/j.ymssp.2016.07.009.

Li, C., Luo, S., Cole, C., & Spiryagin, M. (2018). Bolster spring fault detection strategy for heavy haul wagons. *Vehicle System Dynamics*, *56*(10), 1604–1621. https://doi.org/10.1080/00423114.2017.1423090.

Medeiros, L., Silva, P. H. O., Valente, L. d. C., & Nepomuceno, E. G. (2018). A prototype for monitoring railway vehicle dynamics using inertial measurement units. In *2018 13th IEEE International Conference on Industry Applications (INDUSCON)*(pp. 149–154). https://doi.org/10.1109/INDUSCON.2018.8627330.

Navas, M. A., Sancho, C., & Carpio, J. (2020). Disruptive Maintenance Engineering 4.0. *International Journal of Quality & Reliability Management*, *37*(6/7), 853–871. https://doi.org/10.1108/IJQRM-09-2019-0304.

Ngigi, R. W., Pislaru, C., Ball, A., & Gu, F. (2012). Modern techniques for condition monitoring of railway vehicle dynamics. *Journal of Physics: Conference Series*, *364*, 012016. https://doi.org/10.1088/1742-6596/364/1/012016.

Palmgren, A., & Ruley, B. (1959). *Ball and roller bearing engineering*(3rd ed.). SKF Industries Inc.

Papaelias, M., Amini, A., Huang, Z., Vallely, P., Dias, D. C., & Kerkyras, S. (2016). Online condition monitoring of rolling stock wheels and axle bearings. *Proceedings of the Institution of Mechanical Engineers, Part F: Journal of Rail and Rapid Transit*, *230*(3), 709–723. https://doi.org/10.1177/0954409714559758.

Rilling, G., Flandrin, P., Gonçalves, P., & Lilly, J. M. (2007). Bivariate empirical mode decomposition. *IEEE Signal Processing Letters*, *14*(12), 936–939. https://doi.org/10.1109/LSP.2007.904710.

Sahal, R., Breslin, J. G., & Ali, M. I. (2020). Big data and stream processing platforms for Industry 4.0 requirements mapping for a predictive maintenance use case. *Journal of Manufacturing Systems*, *54*, 138–151. https://doi.org/10.1016/j.jmsy.2019.11.004.

Saidy, C., Valappil, S. P., Matthews, R. M., & Bayoumi, A. (2020). Development of a predictive Maintenance 4.0 platform: Enhancing product design and manufacturing. In A. Ball, L. Gelman, & B. K. N. Rao (Eds.), *Advances in asset management and condition monitoring*(Vol. *166*, pp. 1039–1049). Springer International Publishing. https://doi.org/10.1007/978-3-030-57745-2_86.

Shin, J.-H., & Jun, H.-B. (2015). On condition based maintenance policy. *Journal of Computational Design and Engineering*, *2*(2), 119–127. https://doi.org/10.1016/j.jcde.2014.12.006.

Su, L., Ma, L., Qin, N., Huang, D., & Kemp, A. H. (2019). Fault diagnosis of high-speed train bogie by residual-squeeze net. *IEEE Transactions on Industrial Informatics*, *15*(7), 3856–3863. https://doi.org/10.1109/TII.2019.2907373.

Takikawa, M. (2016). Innovation in railway maintenance utilizing information and communication technology (smart maintenance initiative). *Japan Railway & Transport Review*, *67*, 14.

Thompson, D. (2009). *Railway noise and vibration* (1st ed.). Elsevier. https://doi.org/10.1016/B978-0-08-045147-3.X0023-0.

Thompson, C., Reichl, P., Zeng, D., White, J., Ahmed, F., & Sethi, H. (2016). Predictive maintenance approaches based on continuous monitoring systems at Rio Tinto. In *Proceedings of CORE2016*(p. 7).

Urbanic, R. J., & ElMaraghy, W. (2009). A design recovery framework for mechanical components. *Journal of Engineering Design*, *20*(2), 195–215. https://doi.org/10.1080/09544820701802261.

Urbanic, R. J. (2015). A design and inspection based methodology for form-function reverse engineering of mechanical components. *The International Journal of Advanced Manufacturing Technology*, *81*(9–12), 1539–1562. https://doi.org/10.1007/s00170-015-7180-5.

van Staden, H. E., & Boute, R. N. (2021). The effect of multi-sensor data on condition-based maintenance policies. *European Journal of Operational Research*, *290*(2), 585–600. https://doi.org/10.1016/j.ejor.2020.08.035.

Xie, X. (2008). A review of recent advances in surface defect detection using texture analysis techniques. *ELCVIA Electronic Letters on Computer Vision and Image Analysis*, *7*(3), 1. https://doi.org/10.5565/rev/elcvia.268.

Yun, Z., Zhi-Tong, C., & Tao, N. (2015). Reverse modeling strategy of aero-engine blade based on design intent. *The International*

Journal of Advanced Manufacturing Technology, *81*(9–12), 1781–1796. https://doi.org/10.1007/s00170-015-7232-x.

Zasiadko, M. (2019, July 16). *Deutsche Bahn produces heavy spare parts on 3D printer | RailTech.com*. RailTech.Com | Online News for the Railway Industry. https://www.railtech.com/digitalisation/2019/07/16/deutsche-bahn-produces-heavy-spare-parts-on-3d-printer/.

Zhang, Y., Chen, Z.-T., & Ning, T. (2016). Efficient measurement of aero-engine blade considering uncertainties in adaptive machining. *The International Journal of Advanced Manufacturing Technology*, *86*(1–4), 387–396. https://doi.org/10.1007/s00170-015-8155-2.

Zhao, F., Xu, X., & Xie, S. Q. (2009). Computer-aided inspection planning—The state of the art. *Computers in Industry*, *60*(7), 453–466. https://doi.org/10.1016/j.compind.2009.02.002.

Zougari, A., Martínez, J., & Cardona, S. (2016). Numerical models of railway tracks for obtaining frequency response comparison with analytical results and experimental measurements. *Journal of Vibroengineering*, *18*(2), 11.